ELSEVIER

21 July 1997

PHYSICS LETTERS A

Physics Letters A 232 (1997) 41–48

Input–output gains for signal in noise in stochastic resonance

François Chapeau-Blondeau

Laboratoire d'Ingénierie des Systèmes Automatisés (LISA), Faculté des Sciences, Université d'Angers, 2 boulevard Lavoisier, 49000 Angers, France

Received 10 March 1997; accepted for publication 21 April 1997
Communicated by C.R. Doering

Abstract

A theoretical model for the transmission of a periodic signal added to a noise through a static nonlinearity is considered. Expressions are derived for the gains experienced by the signal, the noise and the signal-to-noise ratio in the input–output nonlinear transmission. The gains are obtained in the presence of a periodic input, a noise distribution and a static nonlinearity, all three being arbitrary. These gains are studied as measures of the phenomenon of stochastic resonance whereby the transmission of the periodic signal can be improved by means of noise addition. As the noise level is raised, resonant evolutions for the signal and signal-to-noise gains or antiresonant evolutions for the noise gain, are demonstrated. At the same time, conditions are exhibited where the signal-to-noise gain is larger than unity, demonstrating several realizations of a signal-to-noise ratio larger at the output than at the input in stochastic resonance. © 1997 Elsevier Science B.V.

PACS: 05.40.+j; 02.50.−r; 07.50.Qx; 47.20.Ky
Keywords: Stochastic resonance; Signal; Noise; Nonlinear systems; Stochastic processes; Signal processing

1. Introduction

Stochastic resonance is a nonlinear phenomenon whose relevance is gradually extending to a broad class of systems [1,2]. In general terms, stochastic resonance can be defined as an enhancement of the transmission of a coherent signal by a nonlinear system, that is obtained by means of noise addition to the system. This paradoxical effect has now been reported in a large variety of nonlinear systems including lasers [3,4] electronic devices [5,6], neurons [7–9].

So far, the focus has essentially been placed on the transmission of a periodic signal, although stochastic resonance has recently been extended to aperiodic signals [10–12]. Various measures can be used for the efficacy of the transmission process receiving enhancement from the noise. The measures most frequently employed for periodic stochastic resonance are an output signal-to-noise ratio [13–15], or the amplitude of the coherent component in the noisy output [13,16,15]. The possibility of increasing the value of these measures when noise is added is taken as the signature of stochastic resonance. Such an outcome signifies that the detectability of the coherent component in the output signal-plus-noise mixture can be improved by noise addition at the input. Yet, to further assess the potentialities of stochastic resonance leads to the examination of a complementary question: Is it possible to have the detectability of the coherent component in the output signal-plus-noise mixture (shown to be improvable by noise addition at the input) exceed the detectability of the coherent component in the input signal-plus-noise mixture? With the conventional signal-to-noise ratio (SNR) as the measure of

PII S0375-9601(97)00350-2

efficacy, this translates into examining the possibility of a larger SNR at the output than at the input of the stochastic resonator.

This important issue was touched in Refs. [17–19] to result in no positive answer. In Refs. [20,21] proofs were given that, in the limit of a small coherent signal with Gaussian noise, the output SNR cannot exceed that at the input. By circumventing the small-signal limit, Ref. [22] manages to exhibit a stochastic resonator with a SNR larger at the output than at the input. The report in Ref. [22] is based on a numerical simulation of a level-crossing detector driven by a periodic spike train.

In the present work, we use a recently proposed theory that describes stochastic resonance in static nonlinear systems [23]. With this theory, we derive input–output gains for the signal, the noise and the signal-to-noise ratio in the nonlinear transmission. We study the evolutions of these gains with the noise level as measures for stochastic resonance, and focus on conditions allowing a SNR gain larger than unity.

2. Theoretical model

In this section, we briefly review the core of the theory of Ref. [23] and use it to derive expressions for different input–output gains characterizing the stochastic resonators we shall consider in the next sections.

$s(t)$ is a coherent periodic signal with the period T_s. $\eta(t)$ is a stationary white noise with the probability density function $f_\eta(u)$ and the statistical distribution function $F_\eta(u) = \int_{-\infty}^{u} f_\eta(u')\,\mathrm{d}u'$. These two signals form the inputs to a static nonlinear system producing the output

$$y(t) = g[s(t) + \eta(t)], \tag{1}$$

where g is a function operating on real numbers.

The coherent part in the output signal $y(t)$ shows up in the output power spectral density as spectral lines at integer multiples of the coherent frequency $1/T_s$. The power contained in the coherent spectral line at frequency n/T_s is given by $|\overline{Y}_n|^2$, where $\overline{Y}_n$ is the order n Fourier coefficient of the T_s-periodic nonstationary output mean $E[y(t)]$,

$$\overline{Y}_n = \frac{1}{T_s}\int_0^{T_s} E[y(t)]\exp\left(-\mathrm{i}n\frac{2\pi}{T_s}t\right)\mathrm{d}t, \tag{2}$$

where, for a static nonlinearity $g(u)$, the mean $E[y(t)]$ at a fixed time t is computable as

$$E[y(t)] = \int_{-\infty}^{+\infty} g(u) f_\eta[u - s(t)]\,\mathrm{d}u. \tag{3}$$

The incoherent statistical fluctuations in the output signal $y(t)$, which control the continuous noise background in the output power spectral density, are measured by the stationary output variance

$$\overline{\mathrm{var}(y)} = \frac{1}{T_s}\int_0^{T_s} \mathrm{var}[y(t)]\,\mathrm{d}t, \tag{4}$$

where the nonstationary variance $\mathrm{var}[y(t)]$ at a fixed time t is computable as

$$\mathrm{var}[y(t)] = \int_{-\infty}^{+\infty} g^2(u) f_\eta[u - s(t)]\,\mathrm{d}u - \left(\int_{-\infty}^{+\infty} g(u) f_\eta[u - s(t)]\,\mathrm{d}u\right)^2. \tag{5}$$

In the same way, the coherent part at frequency n/T_s in the noisy input $s(t) + \eta(t)$, is measured by the spectral line at frequency n/T_s in the input power spectral density, which contains the coherent power $|S_n|^2$ with the order n Fourier coefficient of $s(t)$,

$$S_n = \frac{1}{T_s}\int_0^{T_s} s(t)\exp\left(-\mathrm{i}n\frac{2\pi}{T_s}t\right)\mathrm{d}t. \tag{6}$$

The ratio of the amplitudes of the output and input coherent spectral lines at frequency n/T_s, which defines the input–output gain G_{sig} for the coherent component at frequency n/T_s, follows as

$$G_{\mathrm{sig}}\left(\frac{n}{T_s}\right) = \frac{|\overline{Y}_n|}{|S_n|}. \tag{7}$$

The incoherent statistical fluctuations in the input $s(t) + \eta(t)$, which control the continuous noise background in the input power spectral density, are

measured by the variance σ_η^2 of the input white noise $\eta(t)$. We define an input–output gain G_{noi} for the amplitude of the noise fluctuations as

$$G_{\mathrm{noi}}\left(\frac{n}{T_s}\right) = \frac{\sqrt{\overline{\mathrm{var}(y)}}}{\sigma_\eta}. \tag{8}$$

The ratio of the output and input SNRs, which defines the input–output gain G_{SNR} for the SNR, follows for the coherent component at frequency n/T_s, as

$$G_{\mathrm{SNR}}\left(\frac{n}{T_s}\right) = \frac{G_{\mathrm{sig}}^2(n/T_s)}{G_{\mathrm{noi}}^2(n/T_s)} = \frac{|\overline{Y}_n|^2/\overline{\mathrm{var}(y)}}{|S_n|^2/\sigma_\eta^2}. \tag{9}$$

The input–output gains of Eqs. (7)–(9) can thus be explicitly computed, from Eqs. (2)–(6), for any periodic waveform $s(t)$ added to any noise distribution $f_\eta(u)$ and transmitted by any nonlinearity $g(u)$. In this model of nonlinear signal transmission, we shall now demonstrate the existence of conditions realizing the double property of (i) a stochastic resonance effect characterized by the gains G_{sig} or G_{SNR} which increase, or the gain G_{noi} which decreases, when the input noise level is raised, and (ii) the obtaining of a gain G_{SNR} larger than unity.

3. Transmission of a pulse train

For a first illustration, we shall consider the case where the nonlinearity $g(u)$ is a hard threshold with $A_y > 0$:

$$\begin{aligned} g(u) &= 0 \quad \text{for } u \leqslant \theta, \\ &= A_y \quad \text{for } u > \theta. \end{aligned} \tag{10}$$

Application of Eq. (10) into Eqs. (3) and (5) leads, respectively, to

$$E[y(t)] = A_y\{1 - F_\eta[\theta - s(t)]\} \tag{11}$$

and

$$\mathrm{var}[y(t)] = A_y^2 F_\eta[\theta - s(t)]\{1 - F_\eta[\theta - s(t)]\}. \tag{12}$$

For the T_s-periodic signal $s(t)$ we choose a train of square pulses of amplitude $A_s > 0$ and duration T,

$$\begin{aligned} s(t) &= A_s \quad \text{for } t \in [0, T[, \\ &= 0 \quad \text{for } t \in [T, T_s[, \end{aligned} \tag{13}$$

whose Fourier coefficients S_n follow from Eq. (6) as

$$S_n = A_s \frac{T}{T_s} \mathrm{sinc}\left(n\pi \frac{T}{T_s}\right) \exp\left(-in\pi \frac{T}{T_s}\right), \tag{14}$$

with the cardinal sine function $\mathrm{sinc}(u) = \sin(u)/u$.

With such a simple $s(t)$ the time integrations in Eqs. (2), (4) can be explicitly performed to yield

$$\overline{Y}_n = A_y \frac{T}{T_s}[F_\eta(\theta) - F_\eta(\theta - A_s)] \,\mathrm{sinc}\left(n\pi \frac{T}{T_s}\right) \times \exp\left(-in\pi \frac{T}{T_s}\right) \tag{15}$$

and

$$\overline{\mathrm{var}(y)} = A_y^2 \left[\frac{T}{T_s} F_\eta(\theta - A_s)[1 - F_\eta(\theta - A_s)] + \left(1 - \frac{T}{T_s}\right) F_\eta(\theta)[1 - F_\eta(\theta)]\right]. \tag{16}$$

The input–output gains of Eqs. (7)–(9) then follow as

$$G_{\mathrm{sig}}\left(\frac{n}{T_s}\right) = \frac{A_y}{A_s}[F_\eta(\theta) - F_\eta(\theta - A_s)], \tag{17}$$

$$G_{\mathrm{noi}}\left(\frac{n}{T_s}\right) = \frac{A_y}{\sigma_\eta}\left[\frac{T}{T_s} F_\eta(\theta - A_s)[1 - F_\eta(\theta - A_s)] + \left(1 - \frac{T}{T_s}\right) F_\eta(\theta)[1 - F_\eta(\theta)]\right]^{1/2} \tag{18}$$

and

$$G_{\mathrm{SNR}}\left(\frac{n}{T_s}\right) = \frac{\sigma_\eta^2}{A_s^2}[F_\eta(\theta) - F_\eta(\theta - A_s)]^2 \times \left[\frac{T}{T_s} F_\eta(\theta - A_s)[1 - F_\eta(\theta - A_s)] + \left(1 - \frac{T}{T_s}\right) F_\eta(\theta)[1 - F_\eta(\theta)]\right]^{-1}. \tag{19}$$

To illustrate the evolutions of these gains, we consider the case where the input noise $\eta(t)$ is zero-mean Gaussian with the distribution function

$$F_\eta(u) = \frac{1}{2}\left[1 + \mathrm{erf}\left(\frac{u}{\sqrt{2}\sigma_\eta}\right)\right], \tag{20}$$

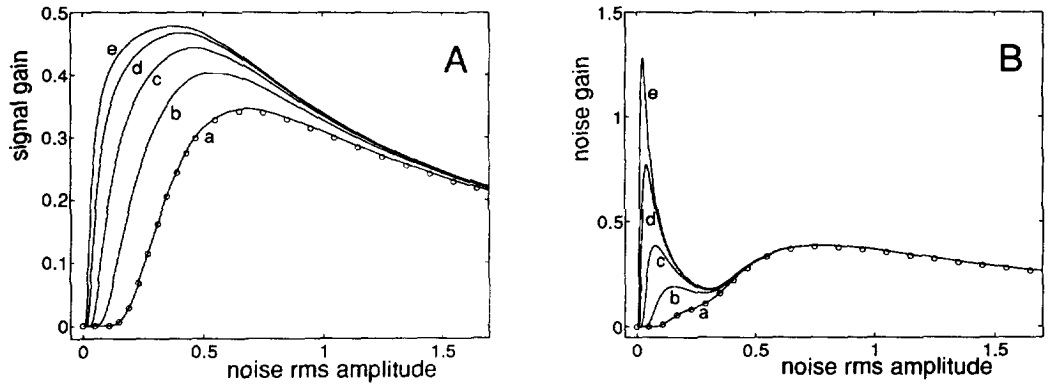

Fig. 1. Input-output gains as a function of the rms amplitude σ_η of the input white noise $\eta(t)$ chosen to be zero-mean Gaussian, with $g(u)$ of Eq. (10) with $\theta = 1$ and $A_y = 1$. The coherent input signal of Eq. (13) is with $T = 10^{-2}T_s$ and (a) $A_s = 0.6$, (b) $A_s = 0.8$, (c) $A_s = 0.9$, (d) $A_s = 0.95$ and (e) $A_s = 0.97$. Panel A is the signal gain $G_{\rm sig}$ from Eq. (17) and panel B the noise gain $G_{\rm noi}$ from Eq. (18). For the case (a) in panels A and B, the set of discrete data points (open circles) results from a numerical simulation of the system.

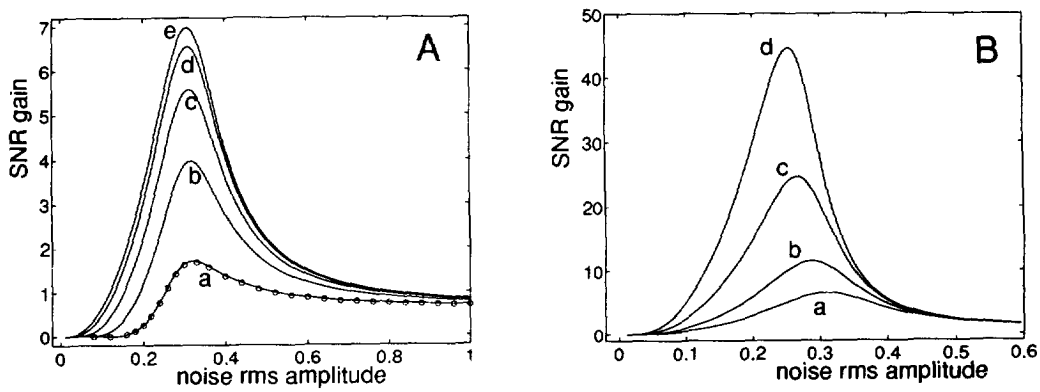

Fig. 2. Input-output SNR gain $G_{\rm SNR}$ from Eq. (19) as a function of the rms amplitude σ_η of the input white noise $\eta(t)$ chosen to be zero-mean Gaussian, with $g(u)$ of Eq. (10) with $\theta = 1$ and $A_y = 1$. Panel A is $G_{\rm SNR}$ corresponding to Fig. 1, with the coherent input signal of Eq. (13) with $T = 10^{-2}T_s$ and (a) $A_s = 0.6$, (b) $A_s = 0.8$, (c) $A_s = 0.9$, (d) $A_s = 0.95$ and (e) $A_s = 0.97$. Panel B is with $A_s = 0.95$ and (a) $T = 10^{-2}T_s$, (b) $T = 5 \times 10^{-3}T_s$, (c) $T = 2 \times 10^{-3}T_s$ and (d) $T = 10^{-3}T_s$. For the case (a) in panel A, the set of discrete data points (open circles) results from a numerical simulation of the system.

with the error function $\mathrm{erf}(u) = 2\int_0^u \exp(-u'^2)\,du' / \sqrt{\pi}$. Figs. 1 and 2 represent the evolutions of the gains with the input noise rms amplitude σ_η, as predicted by the theoretical analysis, for different values of the parameters A_s and T of the periodic input $s(t)$. Numerical and experimental tests can be found in Refs. [23,24] for the theory on which we base the present calculations of the gains. In addition, Figs. 1 and 2 also present results from a numerical simulation of the system, in which we have estimated the quantities $E[y(t)]$ and $\overline{\mathrm{var}(y)}$ that determine the gains, directly from a simulation of $y(t)$ with a very small time step $\Delta t \ll T$. Figs. 1 and 2 show an excellent match between the theoretical and numerical results, since the theoretical analysis is established without approximations.

The results of Fig. 1A clearly show a range where the signal gain $G_{\rm sig}$ increases as the input noise level σ_η increases, up to an optimal noise level where $G_{\rm sig}$ is maximized. Since it takes place at a constant input signal amplitude, the resonant evolution of $G_{\rm sig}$ with σ_η is equivalent to a resonant evolution of the output signal amplitude with σ_η. Further, the present model gives us the possibility to observe that the noise gain $G_{\rm noi}$ can undergo an "antiresonant" evolution, with a range where $G_{\rm noi}$ can decrease as the input noise level

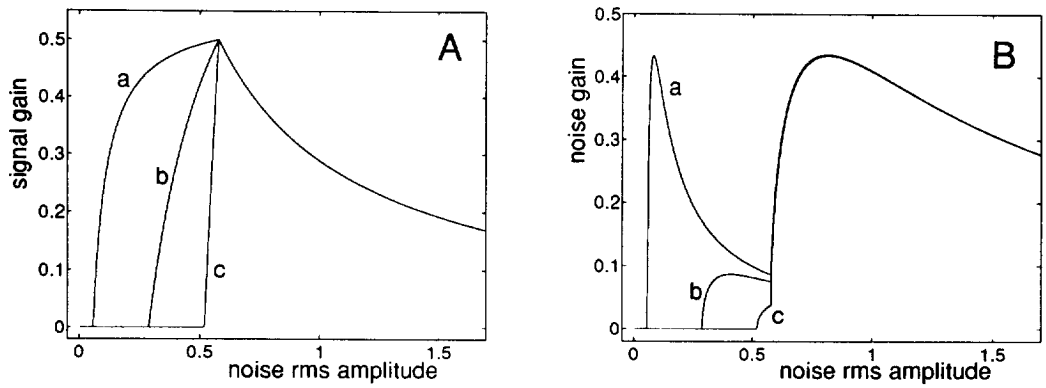

Fig. 3. Input–output gains as a function of the rms amplitude σ_η of the input white noise $\eta(t)$ chosen to be zero-mean uniform, with $g(u)$ of Eq. (10) with $\theta = 1$ and $A_y = 1$. The coherent input signal of Eq. (13) is with $T = 10^{-2}T_s$ and (a) $A_s = 0.9$, (b) $A_s = 0.5$ and (c) $A_s = 0.1$. Panel A is the signal gain G_{sig} from Eq. (17), and panel B the noise gain G_{noi} from Eq. (18).

is raised, as visible in Fig. 1B. We did not find it possible, for the output noise level measured by $\sqrt{\text{var}(y)}$ from Eq. (16) to decrease as the input noise level σ_η increases. Yet, it is quite possible to have $\sqrt{\text{var}(y)}$ which increases more slowly than σ_η, and more and more slowly as σ_η increases. This translates into a gain G_{noi} which decreases as σ_η increases. We note that the absolute values of the gains G_{noi} and G_{sig}, especially relative to 1, have no intrinsic meaning since these values can be directly controlled by A_y in Eqs. (18) and (17). What matters here is the nonmonotonic evolutions of these gains with the input noise level.

The evolutions of the gains G_{noi} and G_{sig} combine, according to Eqs. (9) and (19), to yield a resonant evolution of the SNR gain G_{SNR} with the input noise rms amplitude, as visible in Fig. 2 in various conditions. What is also remarkable in Fig. 2 is the possibility of obtaining a SNR gain larger than unity, proving the ability of the present stochastic resonator to deliver a larger SNR at the output than at the input. As also observed in Ref. [22], the SNR gain gets higher when the filling factor T/T_s of the coherent input gets smaller (Fig. 2B). In order to obtain $G_{\text{SNR}} > 1$, our resonator, as that of Ref. [22], operates in the large-signal regime where the signal amplitude A_s is higher than the noise rms amplitude σ_η. This conforms with the proofs of Refs. [20,21] that, with Gaussian noise and in the small-signal regime, the SNR gain can never be made larger than 1. The large-signal regime is one way to circumvent the limitation of the proofs of Refs. [20,21]. In the following, we show that abandoning the Gaussianity of the noise is another way.

The present model has the ability to describe the influence of the distribution of the input noise $\eta(t)$ on the input–output gains. For illustration, Figs. 3 and 4 show the gains when $\eta(t)$ is a zero-mean uniform noise. Complex influences of the parameters of the system are revealed on the gains. For instance, with the uniform noise G_{SNR} increases as A_s decreases (Fig. 4A), while with the Gaussian noise G_{SNR} increases with A_s (Fig. 2A). The results of Fig. 4A(c) and Fig. 4B show the possibility of $G_{\text{SNR}} > 1$ in the small-signal regime (A_s sufficiently smaller than σ_η), when the noise ceases to be Gaussian.

4. Transmission of a sine wave

To show the possibility of a SNR gain G_{SNR} larger than unity in the transmission of a sine wave, we consider the two-threshold nonlinearity with $\theta > 0$:

$$\begin{aligned} g(u) &= -1 \quad \text{for } u < -\theta, \\ &= 0 \quad \text{for } -\theta \leqslant u \leqslant \theta, \\ &= 1 \quad \text{for } u > \theta. \end{aligned} \tag{21}$$

Application of Eq. (21) into Eqs. (3) and (5) leads, respectively, to

$$E[y(t)] = 1 - F_\eta[\theta - s(t)] - F_\eta[-\theta - s(t)] \tag{22}$$

and

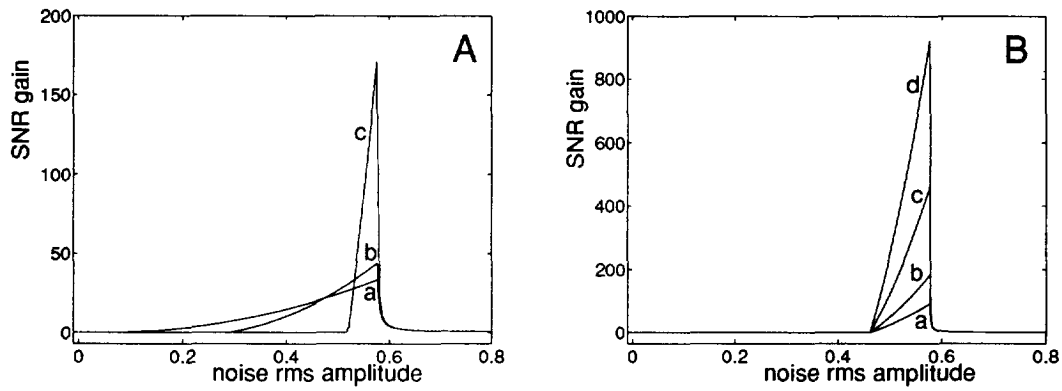

Fig. 4. Input–output SNR gain G_{SNR} from Eq. (19) as a function of the rms amplitude σ_η of the input white noise $\eta(t)$ chosen to be zero-mean uniform, with $g(u)$ of Eq. (10) with $\theta = 1$ and $A_y = 1$. Panel A is G_{SNR} corresponding to Fig. 3, with the coherent input signal of Eq. (13) with $T = 10^{-2}T_s$ and (a) $A_s = 0.9$, (b) $A_s = 0.5$ and (c) $A_s = 0.1$. Panel B is with $A_s = 0.2$ and (a) $T = 10^{-2}T_s$, (b) $T = 5 \times 10^{-3}T_s$, (c) $T = 2 \times 10^{-3}T_s$ and (d) $T = 10^{-3}T_s$.

$$\begin{aligned}\mathrm{var}[y(t)] &= \{1 - F_\eta[\theta - s(t)]\}F_\eta[\theta - s(t)] \\ &+ \{1 - F_\eta[-\theta - s(t)]\}F_\eta[-\theta - s(t)] \\ &+ 2\{1 - F_\eta[\theta - s(t)]\}F_\eta[-\theta - s(t)]. \qquad (23)\end{aligned}$$

With the sine wave $s(t) = A_s\cos(2\pi t/T_s)$, the Fourier coefficients S_n of Eq. (6) reduce to $S_{\pm 1} = A_s/2$, and the time integrations in Eqs. (2), (4) have usually to be performed numerically for a given $F_\eta(u)$. The values of the input–output gains then follow from Eqs. (7)–(9) and are represented in Figs. 5 and 6.

With a Gaussian $\eta(t)$, in contrast to the case of the pulse train $s(t)$ shown in Fig. 2, we did not find it possible, with a sinusoidal $s(t)$ and $g(u)$ of Eq. (21), to observe a SNR gain G_{SNR} larger than unity. Yet, this became quite possible with a uniform $\eta(t)$ as shown by the results of Fig. 6.

To have a concise view of the influence of the distribution of the noise $\eta(t)$ on the input–output gains, it is interesting to consider for $\eta(t)$ the family of centered distributions obtained by passing a zero-mean unit-variance Gaussian noise $\xi(t)$ through the transformation $\eta = A_\eta\,\mathrm{erf}(\beta\xi/\sqrt{2})$ parameterized by $A_\eta > 0$ and $\beta > 0$. This results in a noise $\eta(t)$ with the probability density function

$$\begin{aligned}f_\eta(u) &= \frac{1}{2\beta A_\eta}\exp\left\{\left(1 - \frac{1}{\beta^2}\right)\left[\mathrm{erf}^{-1}\left(\frac{u}{A_\eta}\right)\right]^2\right\} \\ &\qquad \text{for } u \in\,]-A_\eta, A_\eta[, \\ &= 0 \qquad \text{otherwise,} \qquad (24)\end{aligned}$$

and the distribution function

$$\begin{aligned}F_\eta(u) &= 0 \qquad \text{for } u \in\,]-\infty, -A_\eta], \\ &= \frac{1}{2}\left\{1 + \mathrm{erf}\left[\frac{1}{\beta}\mathrm{erf}^{-1}\left(\frac{u}{A_\eta}\right)\right]\right\} \\ &\qquad \text{for } u \in\,]-A_\eta, A_\eta[, \\ &= 1 \qquad \text{for } u \in [A_\eta, +\infty[. \qquad (25)\end{aligned}$$

Varying β from 0 to $+\infty$ allows us to implement a large variety of distributions for $\eta(t)$. For $\beta \ll 1$, $\eta(t)$ tends to a Gaussian noise with rms amplitude $A_\eta\beta\sqrt{2/\pi}$. For $\beta = 1$, $\eta(t)$ is a uniform noise over $]-A_\eta, A_\eta[$. For $\beta \gg 1$, $\eta(t)$ tends to concentrate around the two modes $-A_\eta$ and A_η, and at the limit $\beta = +\infty$, $\eta(t)$ becomes a dichotomous noise with two discrete levels $\{-A_\eta, A_\eta\}$.

As we mentioned, for $\beta \ll 1$, when $\eta(t)$ is close to a Gaussian noise, the maximum SNR gain G_{SNR} at the resonance remains below 1. But as β increases, the maximum G_{SNR} rapidly exceeds 1. As soon as $\beta \sim 1$, when $\eta(t)$ is close to a uniform noise, maximum G_{SNR}'s well above 1 can be obtained, as visible in Fig. 6A. As β is further increased above 1, the

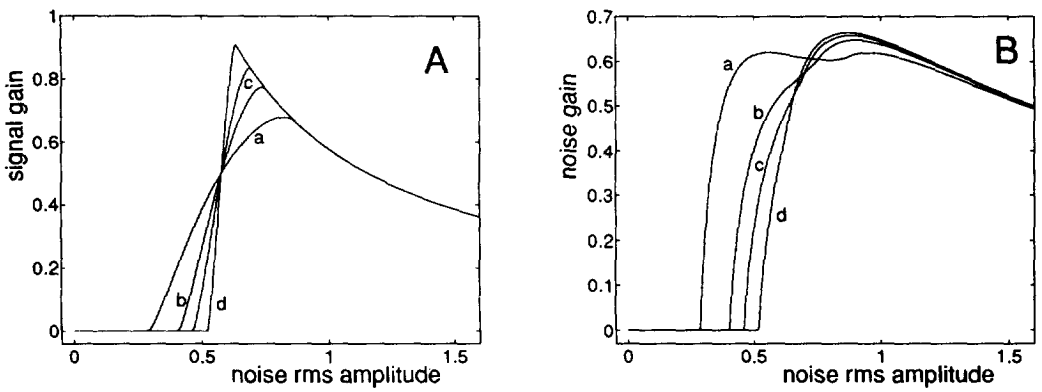

Fig. 5. Input–output gains as a function of the rms amplitude σ_η of the input white noise $\eta(t)$ chosen to be zero-mean uniform, with $g(u)$ of Eq. (21) and $\theta = 1$. The coherent input is the sinusoid $s(t) = A_s \cos(2\pi t/T_s)$ with (a) $A_s = 0.5$, (b) $A_s = 0.3$, (c) $A_s = 0.2$ and (d) $A_s = 0.1$. Panel A is the signal gain G_{sig} from Eq. (7) and panel B the noise gain G_{noi} from Eq. (8).

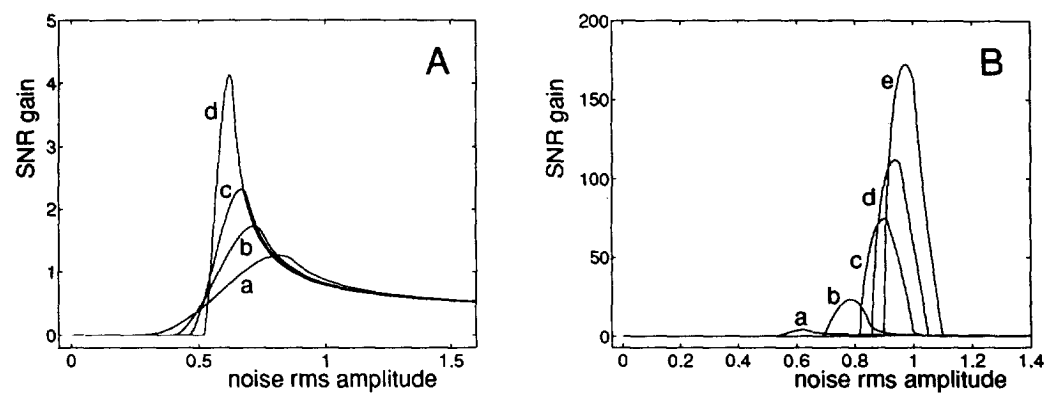

Fig. 6. Input–output SNR gain G_{SNR} from Eq. (9) as a function of the rms amplitude σ_η of the input white noise $\eta(t)$, with $g(u)$ of Eq. (21) with $\theta = 1$ and a sinusoidal coherent input $s(t) = A_s \cos(2\pi t/T_s)$. Panel A is G_{SNR} corresponding to Fig. 5, with (a) $A_s = 0.5$, (b) $A_s = 0.3$, (c) $A_s = 0.2$ and (d) $A_s = 0.1$. Panel B is G_{SNR} with $A_s = 0.1$ and when $\eta(t)$ belongs to the family of noises of Eqs. (24), (25) with (a) $\beta = 1$ (uniform noise), (b) $\beta = 2$, (c) $\beta = 5$, (d) $\beta = 10$ and (e) $\beta = +\infty$ (dichotomous noise).

maximum G_{SNR} is raised well above 1, up to $\beta = +\infty$ where G_{SNR} is maximized, as shown in Fig. 6B, for the present system of Eq. (21) with a sinusoidal input $s(t)$. For the case of the dichotomous noise ($\beta = +\infty$), similar results were reported in Ref. [23] showing a SNR gain larger than unity.

5. Discussion

The present study derives theoretical expressions for different input–output gains characterizing the transmission of a signal-plus-noise mixture by static nonlinearities. Complex dependence of these gains with the noise level are revealed, including resonant or antiresonant evolutions, establishing these gains as appropriate measures for the phenomenon of stochastic resonance. Special attention has been devoted to exhibiting conditions realizing the important property, very seldom reported for stochastic resonators, of a SNR gain G_{SNR} larger than unity.

The property of $G_{\text{SNR}} > 1$ is here reported for the transmission of a periodic pulse train by a static nonlinearity. This is the same property that was observed in Ref. [22] with a different stochastic resonator. Ref. [22] operates with a level-crossing detector, whose dynamics involves a stochastic triggering followed by a deterministic resetting under the form of a square pulse emitted at the output. This system

is easy to simulate, but the mixed character of its dynamics makes its theoretical analysis difficult, and the report of Ref. [22] relies on simulation results. In contrast, for the stochastic resonators considered here, we were able to develop a complete theoretical analysis.

As in Ref. [22], we also found here that the SNR gain increases as the pulse duration T within a period T_s (the filling factor) is reduced (see Fig. 2B). The study in Ref. [22], to obtain its results, imposes that the output pulses emitted by the level-crossing detector are of the same duration as the coherent input pulses. This, somehow, amounts to forcing, in an external a priori manner, known characteristics of the coherent input into the random output, what may play a part in the improvement reported in Ref. [22] for the SNR. In contrast, the stochastic resonators we consider here are free from such a priori tuning to some property of the coherent input.

According to Ref. [22], the "spiky" nature of the coherent input is an essential ingredient to obtain an improvement of the SNR by a level-crossing detector, which is unable to improve the SNR of a sinusoidal input. In our study that deals with another type of static resonator, we were able to report SNR gains larger than unity in the transmission of a sinusoidal input, although not with a Gaussian noise in the case considered.

The present results extend the class of systems and the conditions under which stochastic resonators can realize SNR gains larger than unity. A unique feature is that these results are derived here in a general theoretical framework where the gains can be evaluated in the presence of a static nonlinearity, a periodic input and a noise distribution, all three being arbitrary. This provides means for direct examination of the influence of these parameters on the gains and to optimize gain improvements for a complete class of stochastic resonators. Further, this framework is useful to progress in the assessment of the benefits of stochastic resonance for signal processing.

References

[1] K. Wiesenfeld and F. Moss, Nature 373 (1995) 33.
[2] A.R. Bulsara and L. Gammaitoni, Phys. Today 49 (1996) 39.
[3] B. McNamara, K. Wiesenfeld and R. Roy, Phys. Rev. Lett. 60 (1988) 2626.
[4] J.M. Iannelli, A. Yariv, T.R. Chen and Y.H. Zhuang, Appl. Phys. Lett. 65 (1994) 1983.
[5] S. Fauve and F. Heslot, Phys. Lett. A 97 (1983) 5.
[6] V.S. Anishchenko, M.A. Safonova and L.O. Chua, Intern. J. Bifurcation Chaos 2 (1992) 397.
[7] A. Bulsara et al., J. Theor. Biology 152 (1991) 531.
[8] F. Chapeau-Blondeau, X. Godivier and N. Chambet, Phys. Rev. E 53 (1996) 1273.
[9] X. Godivier and F. Chapeau-Blondeau, Europhys. Lett. 35 (1996) 473.
[10] J.J. Collins, C.C. Chow and T.T. Imhoff, Phys. Rev. E 52 (1995) R3321.
[11] A.R. Bulsara and A. Zador, Phys. Rev. E 54 (1996) R2185.
[12] F. Chapeau-Blondeau, Phys. Rev. E 55 (1997) 2016.
[13] B. McNamara and K. Wiesenfeld, Phys. Rev. A 39 (1989) 4854.
[14] L. Gammaitoni, F. Marchesoni, E. Menichella-Saetta and S. Santucci, Phys. Rev. Lett. 62 (1989) 349.
[15] F. Moss, D. Pierson and D. O'Gorman, Intern. J. Bifurcation Chaos 4 (1994) 1383.
[16] P. Jung and P. Hänggi, Phys. Rev. A 44 (1991) 8032.
[17] D.C. Gong et al., Phys. Rev. A 46 (1992) 3243.
[18] D.C. Gong et al., Phys. Rev. E 48 (1993) 4862.
[19] M.E. Inchiosa and A.R. Bulsara, Phys. Rev. E 52 (1995) 327.
[20] M.I. Dykman et al., Nuovo Cimento 17D (1995) 661.
[21] M. DeWeese and W. Bialek, Nuovo Cimento 17D (1995) 733.
[22] K. Loerincz, Z. Gingl and L.B. Kiss, Phys. Lett. A 224 (1996) 63.
[23] F. Chapeau-Blondeau and X. Godivier, Phys. Rev. E 55 (1997) 1478.
[24] X. Godivier and F. Chapeau-Blondeau, Signal Processing 56(3) (1997) in press.